Collagen Features of Dermatofibrosarcoma Protuberans Skin Base on Multiphoton Microscopy

Shulian Wu, PhD[1]👤, Yudian Huang, MFA[2], Zhifang Li, PhD[1], Huaqing Wu, MFA[1], and Hui Li, PhD[1]

Abstract

Dermatofibrosarcoma protuberans is a rare, low-grade skin fibroblastic tumor which tends to recur locally due to its high misdiagnosis. Dermatofibrosarcoma protuberans usually spreads through the intracutaneous and subcutaneous layers into the deep dermis layer in which the main component is collagen. Therefore, alterations in collagen shape and content are important for accurate diagnosis of dermatofibrosarcoma protuberans. In this study, multiphoton microscopy was employed to observe normal human skin and dermatofibrosarcoma protuberans skin. Then, a centerline based on an algorithm that skeletonizes a binary image of fibers was applied to analyze collagen shapes in 2 types of skin. Then, collagen content, including intensity and density, was quantitatively obtained to demonstrate differences between the 2 skin types. Results indicate that collagen shape and density can be considered as auxiliary diagnostic parameters to improve the accuracy of dermatofibrosarcoma protuberans diagnosis.

Introduction

Dermatofibrosarcoma protuberans (DFSP) is an uncommon and low-grade sarcoma of fibroblast, which results in high local recurrence.[1-3] Dermatofibrosarcoma protuberans, which also occurs in children and adolescents, mainly appears in areas on the trunk, such as the arm, back, and neck, and so on. It is a very slowly growing of skin tumor with a slight yellow-brown.[4] Dermatofibrosarcoma protuberans usually presents as reddish with irregular borders or a multinodular appearance.[5] In general, it spreads through the intracutaneous and subcutaneous into the deep dermis, or fat layer. However, the cause of its formation is still unclear until now.

As with all solid tumors, clinical suspicion is confirmed by biopsy and histological diagnosis. In most cases, examination of hematoxylin and eosin (H&E)-stained specimens by light microscopy results in an unequivocal diagnosis. However, DFSP's diagnosis become complex as a result of initial misdiagnosis.[6] Accurate diagnosis requires more time, and as a result, the tumor may be larger in size at the time of next diagnosis.[2] Multiple nonsupportive biopsies prior to definitive

[1] College of Photonic and Electronic Engineering, Fujian Normal University, Fujian Provincial Key Laboratory of Photonic Technology, Key Laboratory of Optoelectronic Science and Technology for Medicine, Ministry of Education, Fuzhou, China
[2] Department of Pathology, Fuzhou First Hospital Affiliated to Fujian Medical University, Fuzhou, China

Corresponding Author:
Zhifang Li, PhD, College of Photonic and Electronic Engineering, Fujian Normal University, Fujian Provincial Key Laboratory of Photonic Technology, Key Laboratory of Optoelectronic Science and Technology for Medicine, Ministry of Education, Fuzhou 350007, China.
Email: lizhifang@fjnu.edu.cn

diagnosis are common in the clinical process for diagnosing this tumor because of its high misdiagnosis rate. Moreover, it is still unclear whether the substance of DFSP tumor exhibits the histological features of a high mitosis rate or changes in the fibrosarcomata. So, some diagnosis via immunostaining is performed in all cases of suspected DFSP.[6,7] Metastasis is rare in DFSP, but it still occurs in the case of multiple failed treatments of the primary lesion or of changes in the fibrosarcomata.[8] So, it is necessary to develop a noninvasive, effective approach for diagnosing DFSP skin. This could be used in clinical practice for improving the probability of a correct diagnosis and minimizing patient discomfort.

Recently, some new optical imaging methods for diagnosing DFSP skin that would offer real-time, accurate detection without damaging normal tissue or causing patient discomfort have been introduced. These optical methods are helpful for diagnosis and evaluation of skin lesions.[9–13] For example, fluorescence technology was used to obtain intensity with emission wavelength to distinguish some skin lesions, including DFSP skin.[9] This study showed that the fluorescence intensity could distinguish skin lesions with elastin crosslinks, flavins, and porphyrins.[9] Fluorescence *in situ* hybridization has been applied for diagnosis and classification DFSP.[10] Optical coherence tomography (OCT) was used to image the conjunction of normal and DFSP skin and then distinguished the adjacent skin.[11] This result illustrated that OCT supported its potential as an adjuvant to clinical diagnosis.[11] A study in reflectance confocal microscopy illustrated that loss of normal "edge papillae" with elongated bright cells corresponds to tumor cells.[12] And second harmonic generation (SHG) showed its collagen orientation and bundle spacing.[13] All these methods have merit in helping to diagnose DFSP skin. Among them, multiphoton microscopy (MPM) provides a tool to noninvasively visualize dynamic events and has been applied to skin diseases with high resolution, deep penetration depth, and low-level damage to biological tissues.[14-16] Collagen, which can be visualized using an MPM base on SHG, is known to have a significant effect on both mammary morphogenesis and tumor progression and plays an important role in maintaining normal cell behavior.[17,18] So, endogenous signals can be visualized by MPM to reveal pathological changes, which, in turn, could be used to evaluate disease progression.

In this study, excised human skin, including normal and DFSP skin, was observed using MPM, and the centerline shape of collagen was mainly analyzed from skeleton images based on a thinning algorithm. Collagen content, including collagen intensity and density, was then calculated to depict DFSP tumor behavior.

Materials and Methods

Samples

Nineteen skin samples with DFSP and normal tissue were obtained from 19 patients aged between 31 and 62 years undergoing excision surgical procedures at Fuzhou First Hospital affiliated with Fujian Medical University. Skin samples taken from patients were confirmed to have DFSP by biopsy. Samples were from the back (7 samples), neck (9 samples), and shoulder (3 samples). All skin samples, including both normal and DFSP tissue, were investigated to demonstrate the collagen structure for characterizing their pathological state. Our protocol was up to the standard approved by all 16 members of the institutional review board governing clinical investigation of human participants (Approval number: L2017-012.) in biomedical research in Fuzhou First Hospital Affiliated to Fujian Medical University. Informed consent was orally obtained from all patients. Each excised sample was divided into 2 parts. One was used for histological analysis for criteria of DFSP in pathology as a comparison. The other was sliced into a thickness of about 50 μm on the slices by freezing microtome immediately and then stored in a −80 degree celsius refrigerator until the MPM experiment. Before MPM experiments, samples were placed under a cover glass for imaging. To avoid dehydration or shrinkage of samples during the experiment, a few drops of phosphate-buffered solution were added before observation.

Multiphoton Microscopy System

The experimental system employed in this study has been described previously.[13] Our MPM system is a commercial device combined with an Axiovert 200 inverted microscope with Zeiss LSM 510 META laser scanning microscopy (Carl Zeiss Microscopy GmbH, Jena, Germany) and a Coherent Mira 900-F mode-locked femtosecond Ti: sapphire laser (Coherent Inc, Santa Clara, California) (110 fs, 76 MHz) with tunable wavelengths ranging from 700 to 980 nm. The excitation wavelength at 810 nm was used with an average power of about 10 mW. Two objectives with Plan-Neofluar 10 × (Numerical aperture 0.3, Zeiss), and oil immersion objective of Plan-Apochromat 63 × (Numerical aperture 1.4, Zeiss) were employed. Second harmonic generation signal was detected at 404 nm with a bandwidth of 20 nm, while autofluorescence (AF) signal was detected from 430 to 714 nm.

Collagen Characteristic Analysis

Collagen is an important and abundant extracellular matrix component that generates intrinsic contrast via SHG, which has been used to visualize collagen structures as an indicator for many disease states.[19] Collagen fiber shape and collagen content have been used to identify the degree of tissue abnormality, as the shape is key to characterizing abnormal tissue.[20] Researchers have used some methods to obtain collagen shape or alignment.[21,22]

In our study, collagen shape, which skeletonized a binary fiber image, was derived from a centerline-based algorithm in MATLAB R2009b (v7.9.0.529). Otsu threshold is an unbiased threshold that optimizes the ratio of between-group to within-group variance, and it was employed to generate the binary image and to segment the fiber bundles.[23] Binary images of
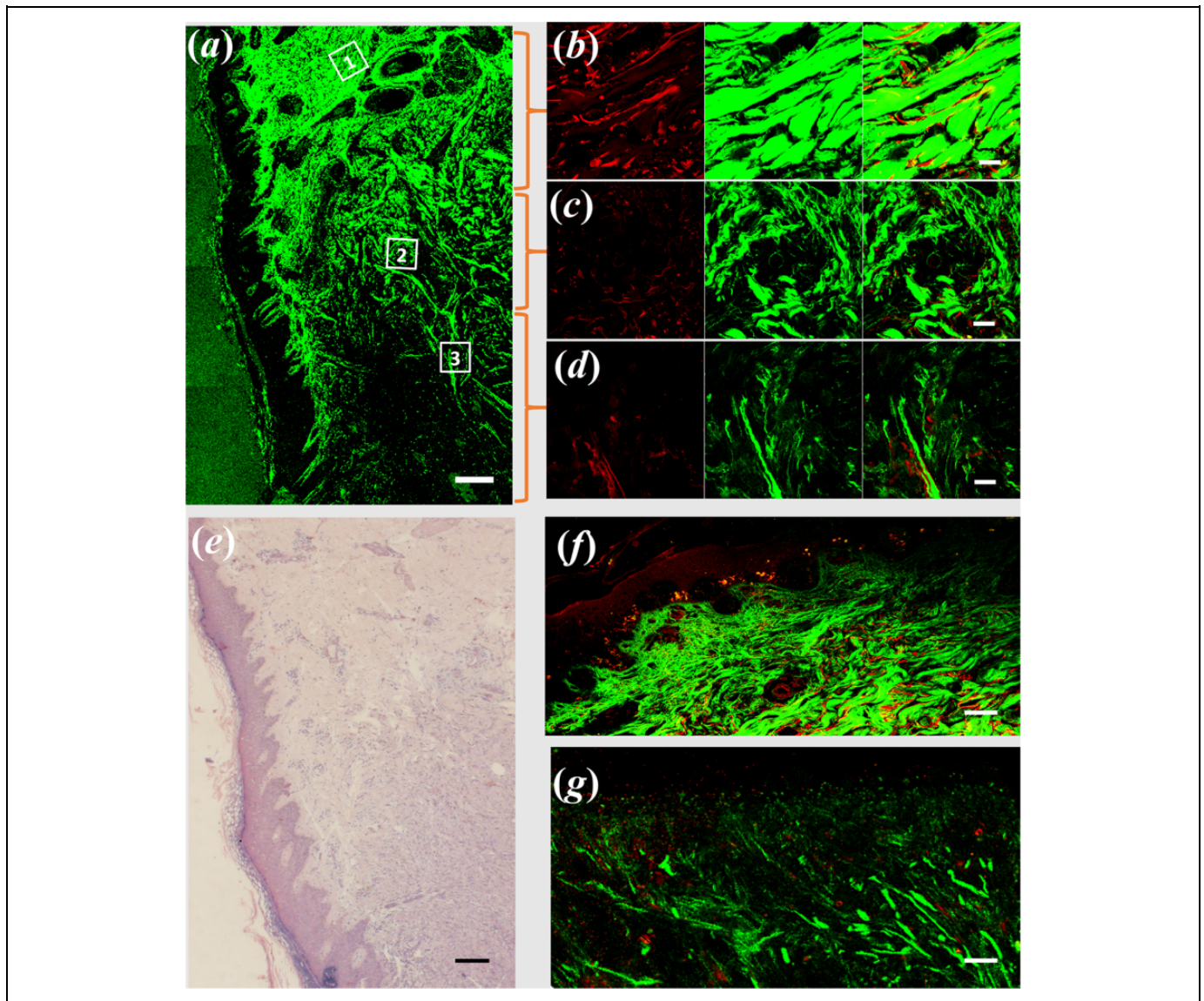
Figure 1. Structure of normal skin and dermatofibrosarcoma protuberans (DFSP) skin, (A) second harmonic generation (SHG) images including the normal (upper) and DFSP skin (down) obtained by the 10× objective. The scale bar is 200 μm. (B-D) Images obtained by the 63× objective. (B) Normal skin from 1 of (A); (C) Conjunction area between normal and DFSP skin from 2 of (A); (D) DFSP skin from 3 of (A). The first column is the autofluorescence (AF) image, second column is SHG image, and the third column is combination. The scale bar is 20 μm. (E) Hematoxylin and eosin (H&E)-stained image corresponding with (A), the scale bar is 200 μm. (F) Epidermis and dermis with combined AF and SHG images in normal skin obtained by the 63× objective. The scale bar is 50 μm. (G) Epidermis and dermis with combined AF and SHG images in DFSP skin obtained by the 63× objective. The scale bar is 50 μm.

fiber bundles were then shrunk to a centerline based on the thinning algorithm to become a skeletonized image.[24]

Collagen density, a parameter for testing collagen content, is an important component of skin tissue.[25] Collagen density reflects quantitative changes in collagen from abnormal tissue. The collagen density value was obtained by dividing the number of pixels containing collagen to the total number of pixels within region of interest (ROI) in the SHG images. It only contains collagen in second harmonic generation images. While AF information, including the other endogenous fluorophores, was displayed with black in the SHG images.

Statistical Analysis

Due to the different optical parameters in different types of skin, detectable strongest intensity layers in different position, the strongest collagen intensity layer was taken as ROI position for collagen content analysis. Five images in the strongest intensity position of ROIs in each sample were selected for quantitative analysis of the strongest collagen intensity and density. One series of images of layer scanning was obtained for analysis from each sample, for each type of skin. Experimental data were processed by statistical testing using SPSS 15.0 software (SPSS Inc, Chicago, Illinois). Statistical
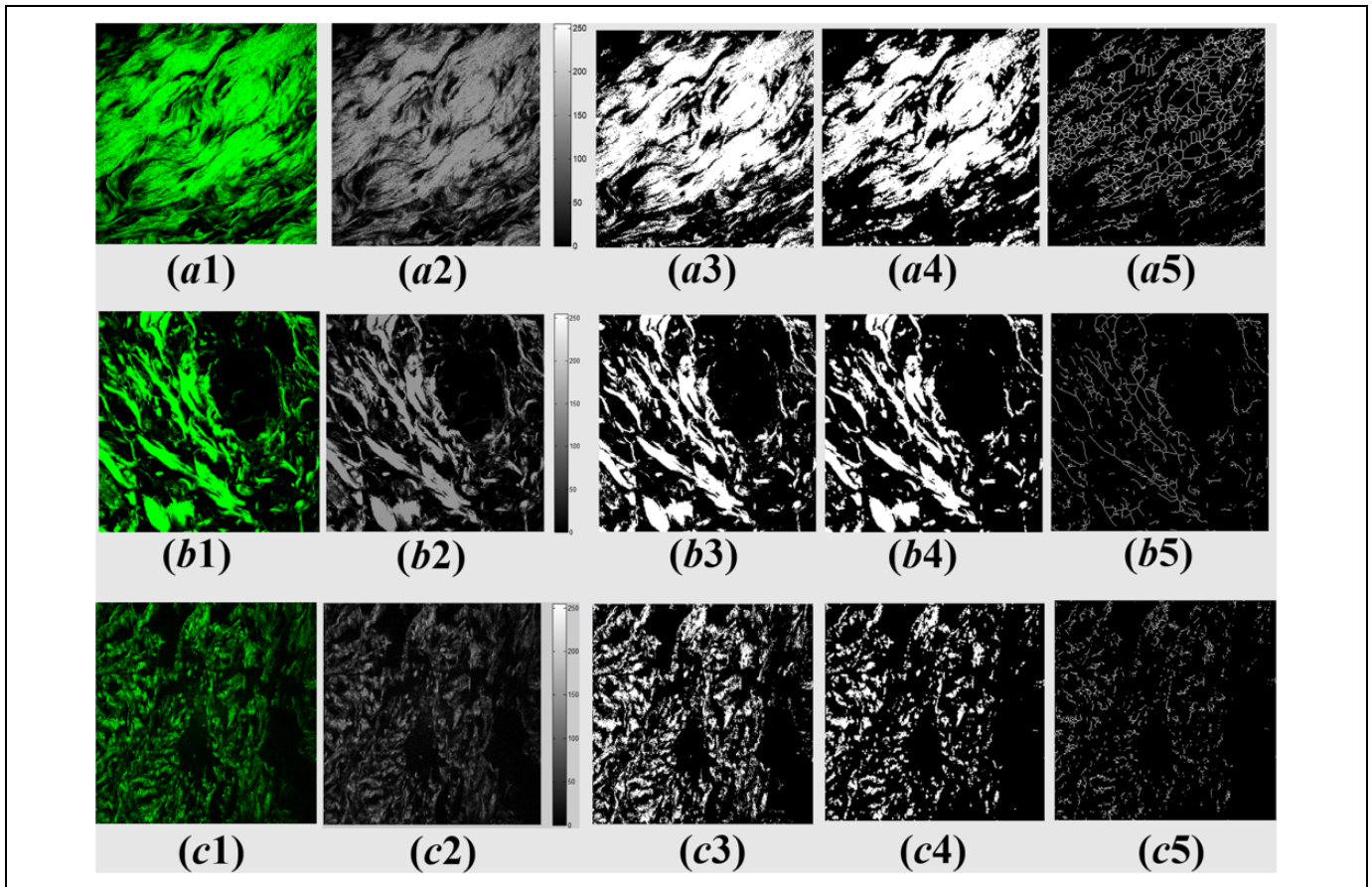
Figure 2. Collagen shape processing. (A1) A normal skin image obtained from $63\times$ objective; (A2) gray image of normal skin; (A3) binary of the normal skin image; (A4) filtered image of normal skin; (A5) skeleton image of the normal skin. (B1) A lesion edge image; (B2) gray image of (B1); (B3) the binary image of (B1); (B4) filter image of (B1); (B5) skeleton image of (B1). (C1) A dermatofibrosarcoma protuberans (DFSP) skin image; (C2) gray image of DFSP image; (C3) binary of DFSP image; (C4) filtered image of DFSP skin; (C5) skeleton image of DFSP skin.

significance of data in different skin types was evaluated using a *t* test to determine whether or not significant differences exist between means of 2 independent groups. Differences were considered statistically significant at $P < .05$.

Results and Discussion

Normal and DFSP Skin Collagen Structure

Collagen morphology is different in each skin type, especially in intensity and fiber shape. Collagen has served as an indicator of tissue lesion, and its character plays an important role in maintaining normal behavior.[26] Collagen structures of normal and DFSP skin are displayed in Figure 1. Images of collagen, including the normal and DFSP skin, were obtained using a $10\times$ objective as shown in Figure 1(A). The normal skin is on the upper part of the figure, and the DFSP skin is on the lower. It can be seen from the figure that the collagen intensity, reflected in the brightness level in the 2 types of skin, differs greatly. To further study collagen intensity, the ROI containing normal, conjunction area, and DFSP skin was obtained with the $63\times$ objective as shown in Figure 1(B), (C), and (D), respectively. The first column contains the AF image; the second column is SHG image, while the third column is the combination images. Autofluorescence images were obtained from intrinsic fluorescence caused by fluorophores such as nicotinamide adenine dinucleotide, elastin, and flavins of skin. While SHG images were mainly obtained from collagen. The images show that the AF signal is weak in deep dermis, while the SHG signal is much stronger. From Figures1(A) to 1(D), we can see that the collagen is generally rod-like, and general differences in collagen shape among the 3 types skin are easy to distinguish.[27,28] It is evident that collagen fibers are bundled in normal skin, collagen bundle became thin in the conjunction area, whereas in DFSP skin the collagen fibers became thinner. These phenomena are caused by the destruction of collagen in DFSP skin. Figure 1(E) was obtained from tissue histology with H&E staining corresponding to Figure 1(A). We can see in the normal part, the collagen is dyed pink, while in DFSP part, the color changes to purple and more cell nucleus was demonstrated. Figure 1(F) and 1(g) show the conjunction of epidermis and dermis in normal skin and DFSP skin, respectively. It can be seen that the epidermis is curved in normal skin, but it is smooth in DFSP skin. This phenomenon is most likely caused by the skin inflammation that makes the skin smooth.
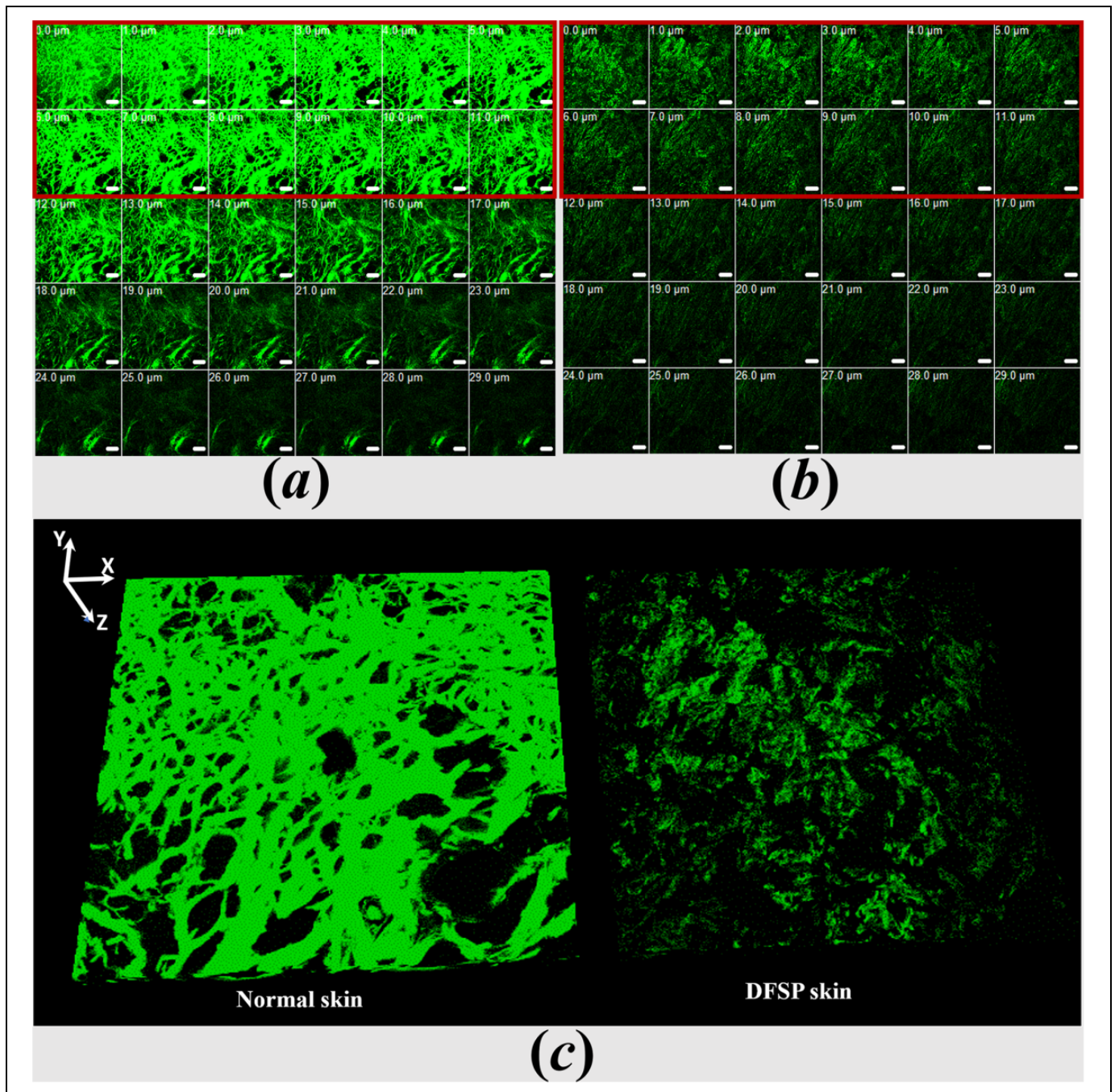
Figure 3. Layer scanning of normal and dermatofibrosarcoma protuberans (DFSP) skin. (A) Second harmonic generation (SHG) images with depth in normal skin (B) DFSP skin. The region of interest (ROI) with red is the focus imaging with the 12-um thick slices. (C) Three dimensions of normal and DFSP skin.

To further understand the changes in collagen fine structure, a centerline-based algorithm was applied to dispose normal and DFSP collagen images. Collagen shape can be used to distinguish the fine structure for normal collagen and abnormal collagen, and the results can be used to predict injury type of patients.[21] The autocalculated fiber orientation method with centerline was described in the "Materials and Methods" section. The centerline method is better at ignoring the crudeness or fineness of collagen fibers as well as collagen dimension,

and the results can be automatically calculated. This makes it the best fit for depicting collagen shape in our study. The disposal process of collagen shape is displayed in Figure 2. Figures 2(A1), 2(B1), and 2(C1) are normal, conjunction area, and DFSP skin images, respectively. Figures 2(A2), 2(B2), and 2(C2) are the gray images of the corresponding of skin. Figures 2(A3), 2(B3), and 2(C3) are the binary images. Figures 2(A4), 2(B4), and 2(C4) are the filtered images. After applying a centerline-based algorithm, skeleton images of collagen were
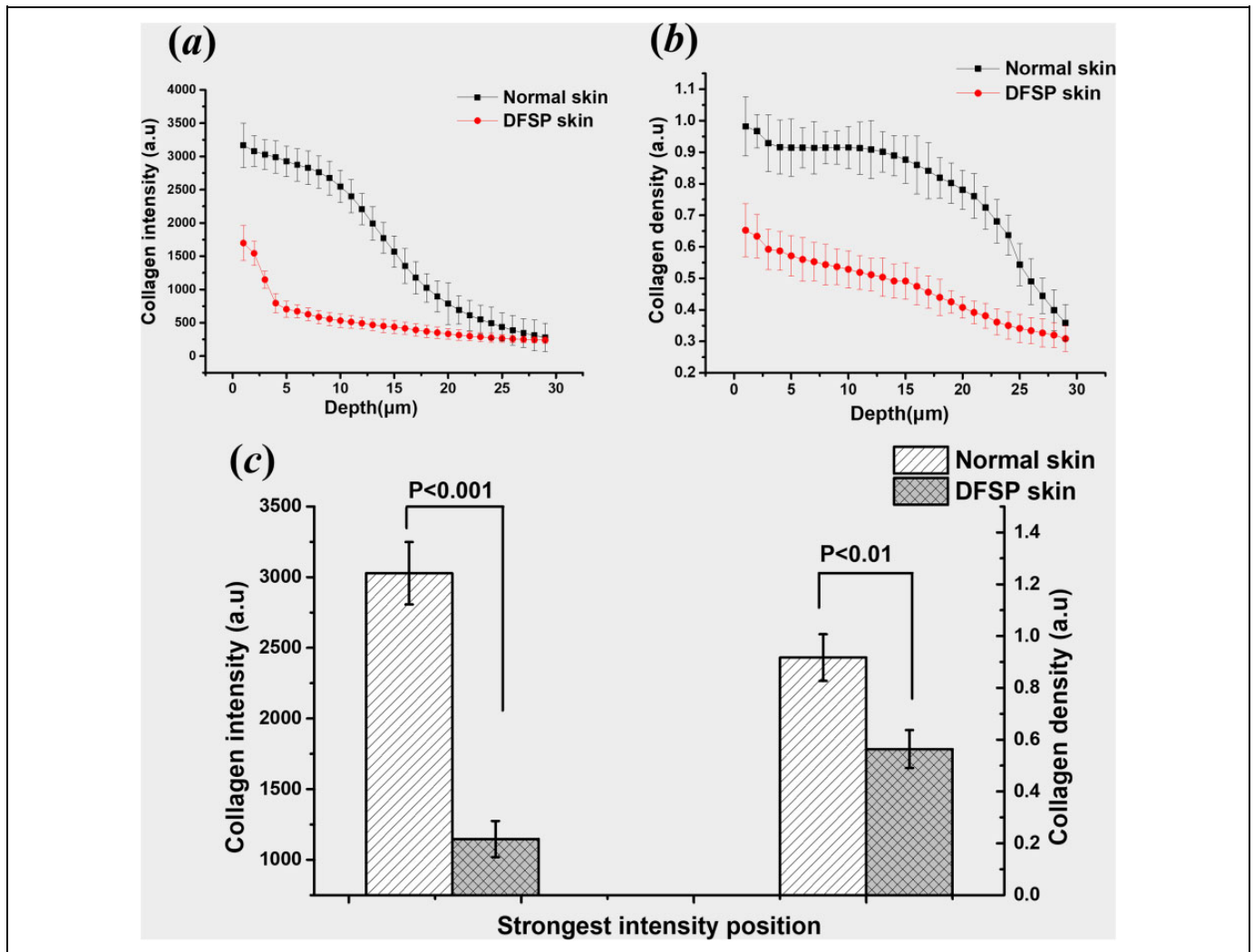
Figure 4. Collagen character of normal and dermatofibrosarcoma protuberans (DFSP) skin. A, Collagen intensity with depth. B, Collagen density with depth. C, Collagen intensity and density at the strongest intensity position of normal skin and DFSP skin.

obtained and are displayed in Figures 2(A5), 2(B5), and 2(C5). From Figures 2 (A1), 2(B1), and 2(C1), it can be observed that collagen is bundled in normal skin, while it is thin in conjunction area, and it becomes thinner, and fractured in DFSP skin. From Figures 2(A5), 2(B5), and 2(C5), centerlines are long, curved, continuous, and intersecting in collagen clusters in normal skin, it become less intersecting and curved in conjunction area, while it is short and nonintersecting in DFSP skin. Results may be caused by the destroyed and fractured collagen. The centerline image can be used to recover the inner alignment and fine differences between normal and DFSP collagen.

Three-Dimensional Structure

For a more graphic description of the changes in collagen structure in DFSP skin, the slice scanning mode was applied to obtain the deeper structure as shown in Figure 3. Due to high scattering in collagen, the detectable signal decayed. The detectable depth is about 30 μm from the strongest intensity,

which is considered as the surface. Thirty layers separated by 1 μm interval of normal skin are shown in Figure 3(A). The strongest signal is located between the first and third layers. The intensity of collagen decreases with depth. Till the first 12 μm, the intensity decreases slightly, as shown in the red line region. After 12 μm, the intensity decreases sharply. The reconstructed 3-D image in normal skin is shown in the left of Figure 3(C), while layer scanning of DFSP skin is shown in Figure 3(B). Collagen signal intensity decreases with depth from the figure, and after 12 μm, the decline degree sharply increases. The 3-D reconstructed image is shown on the right of Figure 3(C). Results more vividly illustrate the collagen distribution in images of the 2 skin types.

Collagen Contents

Microenvironment changes in the tumor are primarily connected with changes in collagen within the tissue stroma, which plays an important role in tumor progression. Quantitatively

analyzed collagen content, including collagen intensity and density, was considered as an optical biomarker to reflect the tumor progression.[29]

Collagen intensity and density changes with detectable depth were calculated and are shown in Figure 4. As shown in Figure 4(A), collagen intensity reduces sharply with depth in both normal skin and DFSP skin. Collagen intensity in normal skin is much higher than in DFSP skin in all layers. The difference at the position with the strongest intensity is shown on the left of Figure 4(C). The relative mean intensity value was about 3100 in normal skin, while it was about 1150 in DFSP. These values have a very significant difference with $P < .001$.

To further outline collagen characteristics, collagen density with detectable depth in the 2 types of skin was extracted and is displayed in Figure 4(B). We can see that the collagen density remains stable in the first 12 layers of normal skin. After that, collagen density decreases sharply with depth. In DFSP skin, collagen density decreases in stability with depth. The difference at the strongest intensity position is shown on the right of Figure 4(C). As shown in the figure, collagen density is about 0.917 in normal skin and decreases sharply to about 0.564 in DFSP skin. The results have statistically significant difference with $P < .01$. Both collagen intensity and density indicate that the collagen content in DFSP decrease sharply, which may cause dermis damage. Collagen fiber is a strong scattering medium, so the detectable signal decreased to about 0 in the deepest depth.

Conclusion

Alteration in collagen changes is the main factor in DFSP skin. In this study, we focused on collagen structure and content in the skin of patients with DFSP using MPM. Results show that in DFSP skin, collagen becomes thinner, and the shape of its centerline becomes more linear and fractal. Collagen content was calculated and indicates that collagen intensity and density decreased sharply in DFSP skin. Results indicate that MPM with collagen autoanalysis can be used as an effective auxiliary tool to diagnose DFSP and reduce misdiagnosis.

Authors' Note

Shulian Wu and Yudian Huang have contributed equally to this study.

Acknowledgments

The authors acknowledge Hannah Horng, from Fischell Department of Bioengineering, University of Maryland, for discussion.

Declaration of Conflicting Interests

The author(s) declared no potential conflicts of interest with respect to the research, authorship, and/or publication of this article.

Funding

ORCID iD

Shulian Wu, PhD http://orcid.org/0000-0002-2572-2320

References

1. Bowne WB, Antonescu CR, Leung DH, et al. Dermatofibrosarcoma protuberans. *Cancer*. 2000;88(12):2711-2720.
2. Mullen JT. Dermatofibrosarcoma protuberans. *Surg Oncol Clin*. 2016;25(4):827-839.
3. Stamatakos M, Fyllos A, Siafogianni A, et al. Dermatofibrosarcoma protuberans: a rare entity and review of the literature. *J BUON*. 2014;19(1):34-41.
4. Tsai YJ, Lin PY, Chew KY, Chiang YC. Dermatofibrosarcoma protuberans in children and adolescents: clinical presentation, histology, treatment, and review of the literature. *J Plast Reconstr Aesthet Surg*. 2014;67(9):1222-1229.
5. Acosta AE, Santa Vélez CS. Dermatofibrosarcoma protuberans. *Curr Treat Options Oncol*. 2017;18(9):56.
6. Lowe GC, Onajin O, Baum CL, et al. A comparison of Mohs micrographic surgery and wide local excision for treatment of dermatofibrosarcoma protuberans with long-term follow-up: The Mayo Clinic experience. *Dermatol Surg*. 2017;43(1):98-106.
7. Tazzari M, Indio V, Vergani B, et al. Adaptive immunity in fibrosarcomatous dermatofibrosarcoma protuberans and response to imatinib treatment. *J Invest Dermatol*. 2017;137(2):484-493.
8. Stacchiotti S, Pantaleo MA, Negri T, et al. Efficacy and biological activity of imatinib in metastatic dermatofibrosarcoma protuberans (DFSP). *Clin Cancer Res*. 2016;22(4):837-846.
9. Ghervase L, Savastru D, Dontu S, Forsea AM, Borisova E. Characterization of human skin by fluorescence, exemplified by dermatofibroma, keratoacanthoma, and seborrheic keratosis. *Anal Lett*. 2016;49(3):342-349.
10. Karanian M, Pérot G, Coindre JM, Chibon F, Pedeutour F, Neuville A. Fluorescence in situ hybridization analysis is a helpful test for the diagnosis of dermatofibrosarcoma protuberans. *Mod Pathol*. 2015;28(2):230-237.
11. Oliveira A, Arzberger E, Zalaudek I, Hofmann-Wellenhof R. Diagnosis of dermatofibrosarcoma protuberans and assessment of pre-surgical margins using high-definition optical coherence tomography imaging. *J Eur Acad Dermatol Venereol*. 2016; 30(4):710-711.
12. Venturini M, Zanca A, Manganoni AM, Pavoni L, Gualdi G, Calzavara-Pinton P. In vivo characterization of recurrent dermatofibrosarcoma protuberans by dermoscopy and reflectance confocal microscopy. *J Am Acad Dermatol*. 2016;75(5): e185-e187.
13. Wu S, Huang Y, Li H, Wang Y, Zhang X. Quantitative analysis on collagen of dermatofibrosarcoma protuberans skin by second harmonic generation microscopy. *Scanning*. 2015;37(1):1-5.
14. Balu M, Kelly KM, Zachary CB, et al. Distinguishing between benign and malignant melanocytic nevi by in vivo multiphoton microscopy. *Cancer Res*. 2014;74(10):2688-2697.

15. Denk W, Strickler JH, Webb WW. Two-photon laser scanning fluorescence microscopy. *Science*. 1990;248(4951):73-76.

16. Zhuo S, Wu G, Chen J, Zhu X, Xie S. Label-free imaging of goblet cells as a marker for differentiating colonic polyps by multiphoton microscopy. *Laser Phys Lett*. 2012;9(6):465-468.

17. Provenzano PP, Eliceiri KW, Campbell JM, Inman DR, White JG, Keely PJ. Collagen reorganization at the tumor-stromal interface facilitates local invasion. *BMC Med*. 2006;4(1):38.

18. Mammoto T, Jiang A, Jiang E, Panigrahy D, Kieran MW, Mammoto A. Role of collagen matrix in tumor angiogenesis and glioblastoma multiforme progression. *Am J Pathol*. 2013;183(4):1293-1305.

19. Campagnola PJ, Dong CY. Second harmonic generation microscopy: principles and applications to disease diagnosis. *Laser Photonics Rev*. 2011;5(1):13-26.

20. Burke KA, Dawes RP, Cheema MK, et al. Second-harmonic generation scattering directionality predicts tumor cell motility in collagen gels. *J Biomed Opt*. 2015;20(5):051024.

21. Matsugaki A, Isobe Y, Saku T, Nakano T. Quantitative regulation of bone-mimetic, oriented collagen/apatite matrix structure depends on the degree of osteoblast alignment on oriented collagen substrates. *J Biomed Mater Res A*. 2015;103(2):489-499.

22. Conklin MW, Eickhoff JC, Riching KM, et al. Aligned collagen is a prognostic signature for survival in human breast carcinoma. *Am J Pathol*. 2011;178(3):1221-1232.

23. Otsu N. Threshold selection method from gray-level histograms. *IEEE Transactions on Systems, Man, and Cybernetics*. 1979;9(1): 62-66.

24. Lam L, Lee SW, Suen CY. Thinning methodologies. *IEEE Transactions on Pattern Analysis and Machine Intelligence*. 1992; 14(9):869-885.

25. Huo CW, Chew G, Hill P, et al. High mammographic density is associated with an increase in stromal collagen and immune cells within the mammary epithelium. *Breast Cancer Res*. 2015;17(1):79.

26. Burke K, Smid M, Dawes R, et al. Using second harmonic generation to predict patient outcome in solid tumors. *BMC Cancer*. 2015;15(1):929.

27. Falzon G, Pearson S, Murison R. Analysis of collagen fibre shape changes in breast cancer. *Phys Med Biol*. 2008;53(23):6641.

28. Hu W, Li H, Wang C, Gou S, Fu L. Characterization of collagen fibers by means of texture analysis of second harmonic generation images using orientation-dependent gray level co-occurrence matrix method. *J Biomed Opt*. 2012;17(2): 0260071-0260079.

29. Uchugonova A, Zhao M, Weinigel M, et al. Multiphoton tomography visualizes collagen fibers in the tumor microenvironment that maintain cancer-cell anchorage and shape. *J Cell Biochem*. 2013;114(1):99-102.